OUKA
The University of Osaka
Institutional Knowledge Archive

Title	Solution properties of a cyclic chain having tunable chain stiffness: Cyclic amylose tris(n-butylcarbamate) in theta and good solvents
Author(s)	Terao, Ken; Shigeuchi, Kazuya; Oyamada, Keiko et al.
Citation	Macromolecules. 2013, 46(13), p. 5355-5362
Version Type	AM
URL	https://hdl.handle.net/11094/81840
rights	This document is the Accepted Manuscript version of a Published Work that appeared in final form in Macromolecules, © American Chemical Society after peer review and technical editing by the publisher. To access the final edited and published work see https://doi.org/10.1021/ma400774r.
Note	

The University of Osaka Institutional Knowledge Archive : OUKA

https://ir.library.osaka-u.ac.jp/

The University of Osaka

Solution Properties of a Cyclic Chain Having Tunable Chain Stiffness: Cyclic Amylose Tris(*n*-butylcarbamate) in Theta and Good Solvents

Ken Terao,,† Kazuya Shigeuchi,† Keiko Oyamada,† Shinichi Kitamura,‡ and Takahiro Sato†*

†Department of Macromolecular Science, Graduate School of Science, Osaka University, 1-1 Machikaneyama-cho, Toyonaka, Osaka 560-0043, Japan.
‡Graduate School of Life and Environmental Sciences, Osaka Prefecture University, Gakuen-cho, Nakaku, Sakai, 599-8531, Japan.
* Corresponding Author. E-mail: kterao@chem.sci.osaka-u.ac.jp

ABSTRACT: Small-angle X-ray scattering measurements were made for nine cyclic amylose tris(*n*-butylcarbamate) (cATBC) samples ranging in the weight-average molar mass M_w from 1.6 $\times$ 10^4 to 1.1 $\times$ 10^5 to determine the *z*-average mean-square radius of gyration $\langle S^2 \rangle_z$ and the particle scattering function $P(q)$ in two good solvents, tetrahydrofuran (THF) and methanol (MeOH) at 25 °C and in a theta solvent, 2-propanol (2PrOH) at the theta temperature (35 °C). Static and dynamic light scattering measurements were carried out for cATBC in 2PrOH to determine M_w, the second virial coefficient A_2, and the hydrodynamic radius R_H. The dimensional and hydrodynamic properties are consistently explained by the current theories for wormlike ring having substantially the same model parameters obtained for linear analogues, that is, the Kuhn segment length λ^{-1} of THF, 2PrOH , and MeOH are 75 nm, 20 nm, and 11 nm, respectively. Furthermore, number of hydrogen bonds decreases with the order of THF, 2PrOH, and MeOH, as is the case with linear ATBC. These results indicate that cATBC has rigid helical backbone stabilized by intramolecular hydrogen bonds in THF and it loosens with increasing solvent polarity. Indeed, lyotropic liquid crystallinity was found for cATBC in THF. In the theta condition, 2PrOH at 35 °C, cATBC has large positive A_2 values, 1.3 – 1.4 $\times$ 10^{-4} mol $g^{-2}cm^3$. It is successfully explained by the simulation results considering intermolecular topological interaction.

■ Introduction

Since cyclic (or ring) polymers have just one more covalent bond between their both ends compared with the corresponding linear polymer, various synthesis methods were developed from several decades ago[1-2] and many kinds of ring polymers have been synthesized recently.[3-6] While theoretical and simulation works for ring polymers have also been performed for the chain dimensions and intermolecular interactions as a function of chain stiffness,[7-8] experimental contributions are mostly limited to flexible chains and few are found for rigid ring polymers instead of cyclic DNA owing to the difficulty of the preparation. Therefore, ring polymers having various chain stiffness should be important to understand their fundamental solution properties and to confirm such theories. Furthermore, such rigid ring chains are of interest as building blocks of supramolecular assemblies.[9-10]

We thus recently demonstrated a new method to obtain a rigid ring polymer, that is, cyclic amylose tris(phenylcarbamate) (cATPC),[11] from rather flexible cyclic amylose[12-14] (or large ring cyclodextrin), which is enzymatically synthesized.[15] Dimensional properties of the obtained

cATPC samples in 1,4-dioxane and 2-ethoxyethanol are well explained by the current theory[16] for the wormlike ring with the same Kuhn segment length λ^{-1} (the chain stiffness parameter, twice of the persistence length) as the corresponding linear amylose tris(phenylcarbamate) (ATPC), that is, 22 nm and 16 nm in 1,4-dioxane and 2-ethoxyethanol,[17] respectively. This chain stiffness is 4 – 5 times higher than that for linear amylose in dimethylsulfoxide.[18] However, the λ^{-1} range of ATPC is quite narrow in the six solvents investigated, that is, 15 – 24 nm.[17,19-20]

On the other hand, we recently found that λ^{-1} for amylose tris(*n*-butylcarbamate) (ATBC) varies much wider range from λ^{-1} = 11 nm in methanol (MeOH) to 75 nm in tetrahydrofuran (THF), and the chain stiffness continuously increases with increasing THF content in THF-MeOH mixed solvent,[21] showing that cyclic ATBC (cATBC, Chart 1) would be a good example as a model ring polymer having tunable chain stiffness. Further important feature is that ATBC has theta solvents, that is, 1-propanol and 2-propanol (2PrOH), in which its λ^{-1} was obtained to be 25 nm and 20 nm, respectively,[22] even though the theta state was seldom found for stiff polymers except for phenylcarbamate derivatives of cellulose and amylose.[19,23]

We therefore prepared cATBC samples from enzymatically synthesized cyclic amylose to investigate their dimensional properties in a theta solvent, 2PrOH, and two good solvents, THF and MeOH, in which the chain stiffness of linear ATBC is the highest and the lowest, respsctively, in the 9 solvents investigated.[21-22,24] Hydrodynamic properties and intermolecular interactions were also investigated in terms of the light scattering method to test the current theories for wormlike rings at and nearby the rigid ring limit.

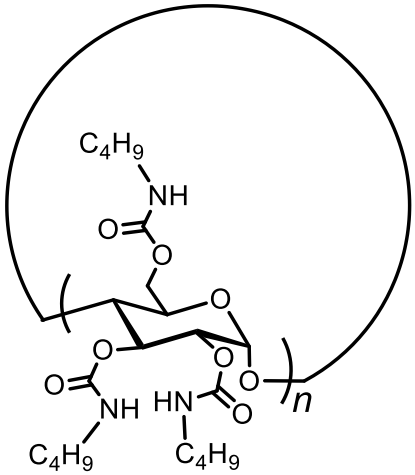

Chart 1. Chemical structure of cyclic amylose tris(*n*-butylcarbamate) (cATBC).

■ Experimental section

Samples and solvents. Cyclic amylose tris(*n*-butylcarbamate) samples were synthesized from four cyclic amylose samples of which weight-average molar mass M_w ranges from 3.1×10^3 to 2.8×10^4 and an excess amount of *n*-butylisocyanate in the similar manner for cATPC[11] and ATBC.[21] The cyclic amylose samples were synthesized enzymatically and purified by using HPLC.[14-15] The reaction mixture was poured into large amount of water to precipitate cATBC. The resultant samples were further purified by successive fractional precipitation to obtain nine samples, cATBC110K, cATBC81K, cATBC75K, cATBC45K, cATBC40K, cATBC37K, cATBC26K, cATBC19K, and cATBC16K. MeOH and water were used as a

solvent and a precipitant, respectively. The degree of substitution was estimated to be 3 ± 0.3 from the mass ratio of carbon to nitrogen determined by elemental analysis. Furthermore, both the ^{1}H NMR and infrared absorption spectra are essentially the same as those for linear ATBC, showing full substitution. Mass spectroscopy was not applied to recognize cyclic polymer contents because of possible (but small amount of) lacking or over substitution of butylcarbamate groups. Anyway, ring opening should be very minor reaction since high molar mass linear ATBC ($M_w \sim 1.6 \times 10^6$) was quantitatively synthesized from linear amylose.[21] Three organic solvents, 2PrOH, MeOH, and THF, for the following measurements were purified by fractional distillation over CaH_2.

Static light scattering (SLS) measurements with size exclusion chromatography (SEC) and static and dynamic light scattering (DLS) measurements. SLS measurements for all samples in THF or MeOH were made by using SEC equipped with a DAWN DSP multi-angle laser light scattering apparatus, a 633 nm laser source, and a refractive index detector under the following condition: A column of Tosoh Multipore-HxLM and flow rate of 1 cm^3min^{-1}. The values of M_w and the ratio of M_w to the number-average molar mass M_n were determined from the scattered intensity and refractive index at each elution volume. It should be noted that unimodal distribution was obtained for all samples.

Conventional SLS and DLS measurements without SEC were made for cATBC81K and cATBC37K in 2PrOH on an ALV/DLS/SLS-5000 light scattering photometer equipped with an ALV-500E/WIN photon correlator at a scattering angle $\theta = 90°$ to determine M_w, the hydrodynamic radius R_H, and the second virial coefficient A_2 as a function of temperature T. The previously reported specific refractive index increments for linear ATBC in the three solvents[21-22] were utilized to analyze the light scattering data. See Figures S1 and S2 in the Supporting Informartion for some raw data for DLS and SLS.

Small-angle X-ray scattering (SAXS) measurements. SAXS measurements were made for cATBC samples in 2PrOH at 35 °C and 17 °C, in MeOH at 25 °C, and in THF at 25 °C to determine the particle scattering function $P(q)$ and the z-average mean-square radius of gyration $\langle S^2 \rangle_z$. Four solutions with different polymer mass concentration c in between 0.001 and 0.02 g cm^{-3} were measured using a 1.5 mmϕ capillary made of quartz glass. The BL40B2 beamline in SPring-8 (Hyogo, Japan) and the BL-10C beamline in KEK-PF (Tsukuba, Japan) were used as X-ray sources. A RIGAKU R-AXIS VII was used as the imaging plate detector. The wavelength, camera length, and accumulation time were set to be 0.10 – 0.15 nm, 1500 – 4000 mm, 150 – 300 sec, respectively. The actual scattering angle at each pixel on the imaging plate was determined by using the Bragg reflection of silver behenate. The obtained scattering data were analyzed by the Guinier plot since theoretical values for rigid ring (equivalent to eq 4 at the limit of $d = 0$) has longer linear region ($\langle S^2 \rangle q^2 < 5$) than that for the Berry and Zimm plots as shown in Figure S3 in the Supporting Information. The experimentally obtained data are summarized in Figure S5. The linear region is narrower than the theoretical values for rigid ring and slight curvature is found even at low-q region for some samples possibly owing to the chain flexibility and/or the polydispersity of our samples. Furthermore, the data nearby the low-q limit might be affected by stray light. Thus, we extrapolated to zero q by taking the data in the range of $\langle S^2 \rangle_z q^2 < 2.5$ into account. At most 6% larger $\langle S^2 \rangle_z$ would be obtained, that is, ~3% for $\langle S^2 \rangle_z^{1/2}$ if we use the data at lower q region.

Infrared Absorption. FT-IR measurements were made for cATBC samples in 2PrOH at 35 °C, MeOH at 25 °C, and THF at 25 °C on an FT/IR 4200 (JASCO) with a solution cell made of CaF_2 having 0.05 mm path length.

■ Results and Discussion

Dimensional Properties and Wormlike Chain Analysis. Table 1 summarizes M_w and M_w/M_n for cATBC samples as well as $\langle S^2\rangle_z^{1/2}$ and R_H in 2PrOH at 35 °C, in MeOH and in THF at 25 °C; we note that $\langle S^2\rangle_z^{1/2}$ and R_H in 2PrOH at 17 °C are substantially the same as those at 35 °C. Molar mass dependences of $\langle S^2\rangle_z^{1/2}$ in the three solvents are summarized in Figure 1 along with those for linear ATBC. The data points for cATBC (unfilled circles) are appreciably smaller than those for linear ATBC (filled circles) at the same M_w, as is the case with our recent results for cATPC.[11] The $\langle S^2\rangle_z^{1/2}$ values in THF are mostly equivalent with the dashed magenta line for rigid ring having finite chain thickness (a torus), of which radius of gyration $\langle S^2\rangle$ can be written as follows

$$\left\langle S^2\right\rangle = \frac{L^2}{4\pi^2} + \frac{d^2}{4} \qquad (1)$$

where L is the contour length (in this case, the circumference) and d is the diameter of the cross section. The former parameter can be related with the molar mass per unit contour length M_L as

$$L = M/M_L \qquad (2)$$

where M is the molar mass of the polymer. In THF, M_L and d were chosen to be 1600 $nm^{-1}g\ mol^{-1}$ and 1.5 nm, respectively. On the other hand, the slope for cATBC in 2PrOH and MeOH are appreciable smaller than that for the theoretical dashed curve for rigid ring, indicating that higher chain flexibility in these two solvents. This smaller slope for cATBC in MeOH comparing with that in THF can be recognized from Figure S6 in the Supporting Information. According to Shimada and Yamakawa, radius of gyration $\langle S^2\rangle_0$ for thin wormlike ring is written as[16]

$$\left\langle S^2\right\rangle_0 = \frac{L^2}{4\pi^2}\left[\begin{array}{l} 1 - 0.1140\,\lambda L - 0.0055258\,(\lambda L)^2 \\ + 0.0022471\,(\lambda L)^3 - 0.00013155\,(\lambda L)^4 \end{array}\right] \quad for \quad \lambda L \le 6$$
$$= \frac{L}{12\lambda}\left\{1 - \frac{7}{6\lambda L} - 0.025\exp\left[-0.01(\lambda L)^2\right]\right\} \quad for \quad \lambda L \ge 6 \qquad (3)$$

This equation is valid even at rigid ring limit if we define λ^{-1} as the bending force constant of the elastic wire divided by k_BT, where k_B is the Boltzmann constant. Thus, the radius of gyration for cylindrical wormlike ring can be estimated by the sum of $\langle S^2\rangle_0$ and $d^2/4$. The three parameters, M_L, λ^{-1}, and d, are unequivocally determined for cATBC in MeOH and 2PrOH from curve fitting procedures, and the resultant theoretical solid curves calculated with the parameters in Table 2 fit the experimental data. The determination error of the obtained λ^{-1} and M_L were estimated from the parameter range that the theoretical values explain the experimental data substantially close to that for the mean value. We suppose that the polydispersity of our samples affects mainly M_L because the dispersity indices are in a rather narrow range between 1.09 and 1.23 and the shape of $\langle S^2\rangle_z - M$ plot for wormlike ring is substantially the same as that for wormlike linear chain.[16] Indeed, in many cases for semiflexible polymers[25] including linear ATBC,[21-22,24] experimentally obtained λ^{-1} from $\langle S^2\rangle_z$ is substantially the same as that from intrinsic viscosity while the M_L from the former method is roughly M_w/M_z times smaller than that from the latter. The obtained λ^{-1} are appreciably larger even in MeOH than that for cyclic

amylose in water[25] (~ 4 nm). Indeed, theoretical values for flexible ring with λ^{-1} = 4 nm have much smaller slope as shown in Figure 1, indicating unmistakable higher chain stiffness of cATBC. It should be noted that the experimental data for cATBC in THF are also well fitted by the theoretical values for wormlike ring with λ^{-1} = 75 nm which is previously determined for linear ATBC, while λ^{-1} in THF cannot be determined from the current $<S^2>_z$ data. If we consider ring polymers having sufficiently long main chain should have the same wormlike chain parameters as the linear chain, we may conjecture from the current result that λ^{-1} for cATBC in THF is as high as 75 nm.

Table 1. Molecular Characteristics and Physical Properties of cATBC Samples in Tetrahydrofuran (THF) at 25 °C, in 2-Propanol (2PrOH) at 35 °C, and in Methanol (MeOH) at 25 °C.

Sample	$10^{-3}M_w$ (g mol^{-1})	M_w / M_n	$<S^2>_z^{1/2}$ (nm)			R_H (nm)
			in THF at 25 °C	in 2PrOH at 35 °C	in MeOH at 25 °C	in 2PrOH at 35 °C
cATBC110K	111	1.23	9.4	9.0	7.8	
cATBC81K	80.9	1.19		7.0	6.3	6.1
cATBC75K	74.6	1.13	7.3			
cATBC45K	44.5	1.22		5.3		
cATBC40K	40.2	1.14	4.4	4.7		
cATBC37K	36.6	1.22	3.9	4.2	3.9	3.9
cATBC26K	26.2	1.12	2.90	3.20		
cATBC19K	18.8	1.10		2.28	2.15	
cATBC16K	16.0	1.09	1.70	1.83	1.80	

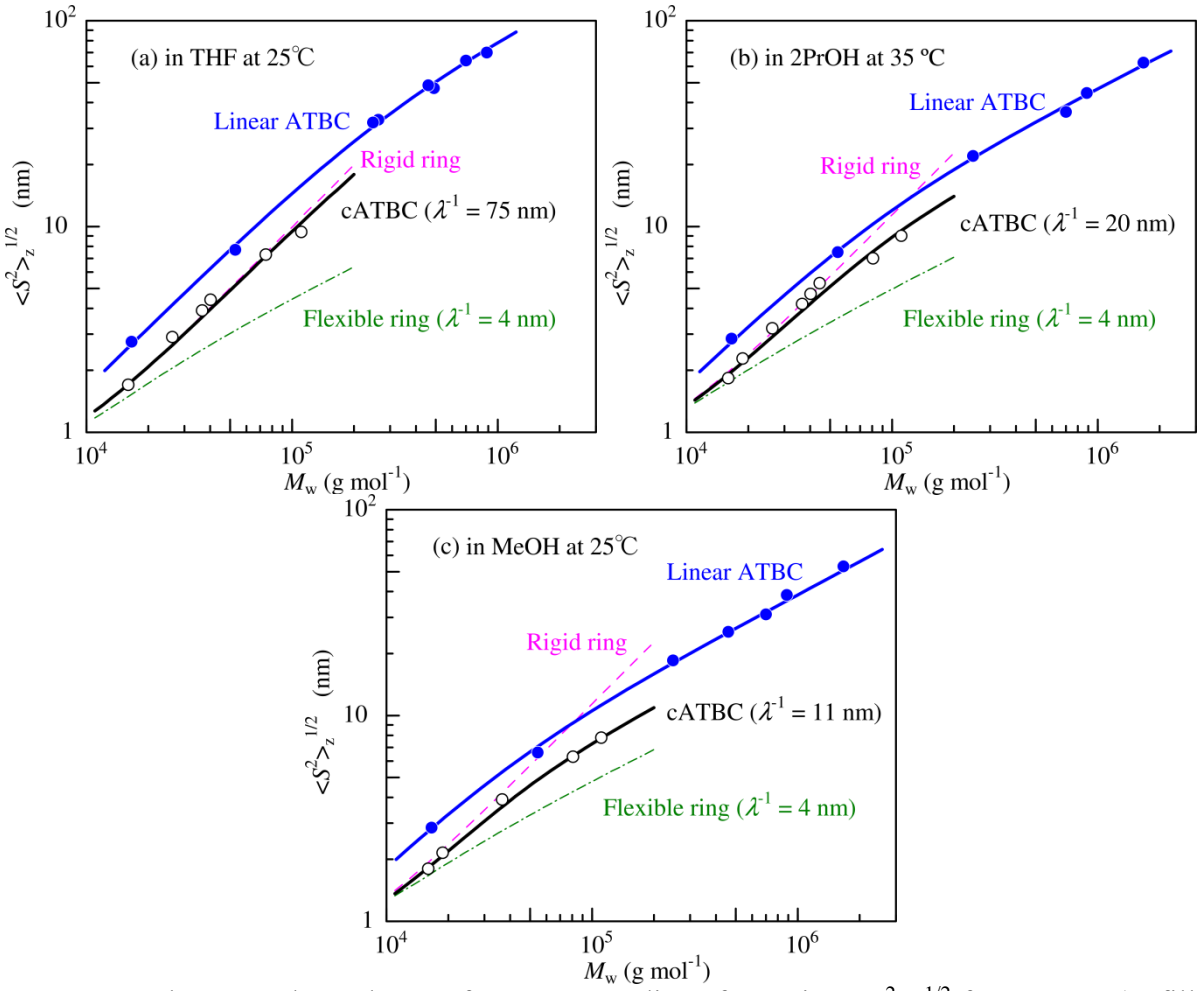

Figure 1. Molar mass dependence of *z*-average radius of gyration $<S^2>_z^{1/2}$ for cATBC (unfilled circles) and linear ATBC[21] (filled circles) in THF at 25 °C (a), in 2PrOH at 35 °C (b), and in MeOH at 25 °C (c). Solid black curves, theoretical values for cylindrical wormlike ring calculated with the parameters listed in Table 2. Dashed (magenta) and dot-dashed (green) lines, theoretical values for rigid ($\lambda^{-1} = \infty$) and rather flexible (λ^{-1} = 4 nm) cyclic cylinders.

Table 2. Molecular Parameters Used for the Calculation of $\langle S^2 \rangle_z$ and $P(q)$ for cATBC in THF at 25 °C , in 2PrOH at 35 °C, and in MeOH at 25 °C.

Physical properties	M_L (nm^{-1}g mol^{-1})	λ^{-1} (nm)	d (nm)
In THF at 25°C			
$\langle S^2 \rangle_z$	1600 ± 50	75*	1.3
$P(q)$	1650 ± 50		1.3
In 2PrOH at 35°C			
$\langle S^2 \rangle_z$	1400 ± 100	20 ± 3	1.5
$P(q)$	1550 ± 50		1.5
In MeOH at 25°C			
$\langle S^2 \rangle_z$	1400 ± 100	11 ± 2	1.3
$P(q)$	1400 ± 50		1.3

* Assumed

Figure 2 summarizes the $P(q)$ data as the Holtzer plots, $q\,P(q)$ vs q. Each plot has an appreciable peak at low q range whereas those for linear ATBC have flat plateau or smaller peak for higher molar mass samples.[21] This is a typical feature for rigid ring polymers.[11] The scattering function $P(q)$ for rigid rings having cylindrical cross section (a torus) can be calculated as

$$P(q) = \int_0^{\pi/2} \left[4J_0\left(\frac{L\,q\sin\xi}{2\pi}\right) J_1\left(\frac{d\,q}{2}\right) \Big/ d\,q \right]^2 \sin\xi\, d\xi \quad (4)$$

where, $J_n(x)$ is the Bessel function of the n-th order. As shown in our previous paper,[11] appreciable fluctuation is found in the calculated $P(q)$ (green dashed curves) for rigid rings even at high q while the experimental $qP(q)$ decreases smoothly. This is likely due to the combined effects of dispersity of molar mass of cATBC and finite chain stiffness. Indeed, if we consider the dispersity by using log normal distribution with M_w/M_n = 1.05 (solid blue curve) and 1.20 (dot-dashed red curve), the fluctuation mostly disappears. The theoretical $qP(q)$ values calculated with the parameters in Table 2 and an appropriate dispersity reproduce the experimental data in 2PrOH and THF for lower M_w samples, but those for the two highest M_w samples in the two solvents and all data in MeOH underestimate at the low q range (< 1 nm^{-1}). This is likely due to the chain flexibility because the discrepancy becomes more appreciable with increasing molar mass and it is also in the order of the chain stiffness, that is, THF < 2PrOH < MeOH. The helix pitch per residue h, defined as $h = M_0/M_L$ can be estimated from average M_L values in Table 2 to be 0.28 nm, 0.31 nm, and 0.33 nm in THF, 2PrOH, and MeOH, respectively. These values are slightly larger than those for linear ATBC (0.26, 0.29, and 0.31 nm), but we may conclude that both the wormlike chain parameters, h and λ^{-1}, for cATBC is essentially the

same as those for linear polymer considering slightly wider molar mass dispersity as well as assumption of log-normal distribution to calculate $P(q)$.

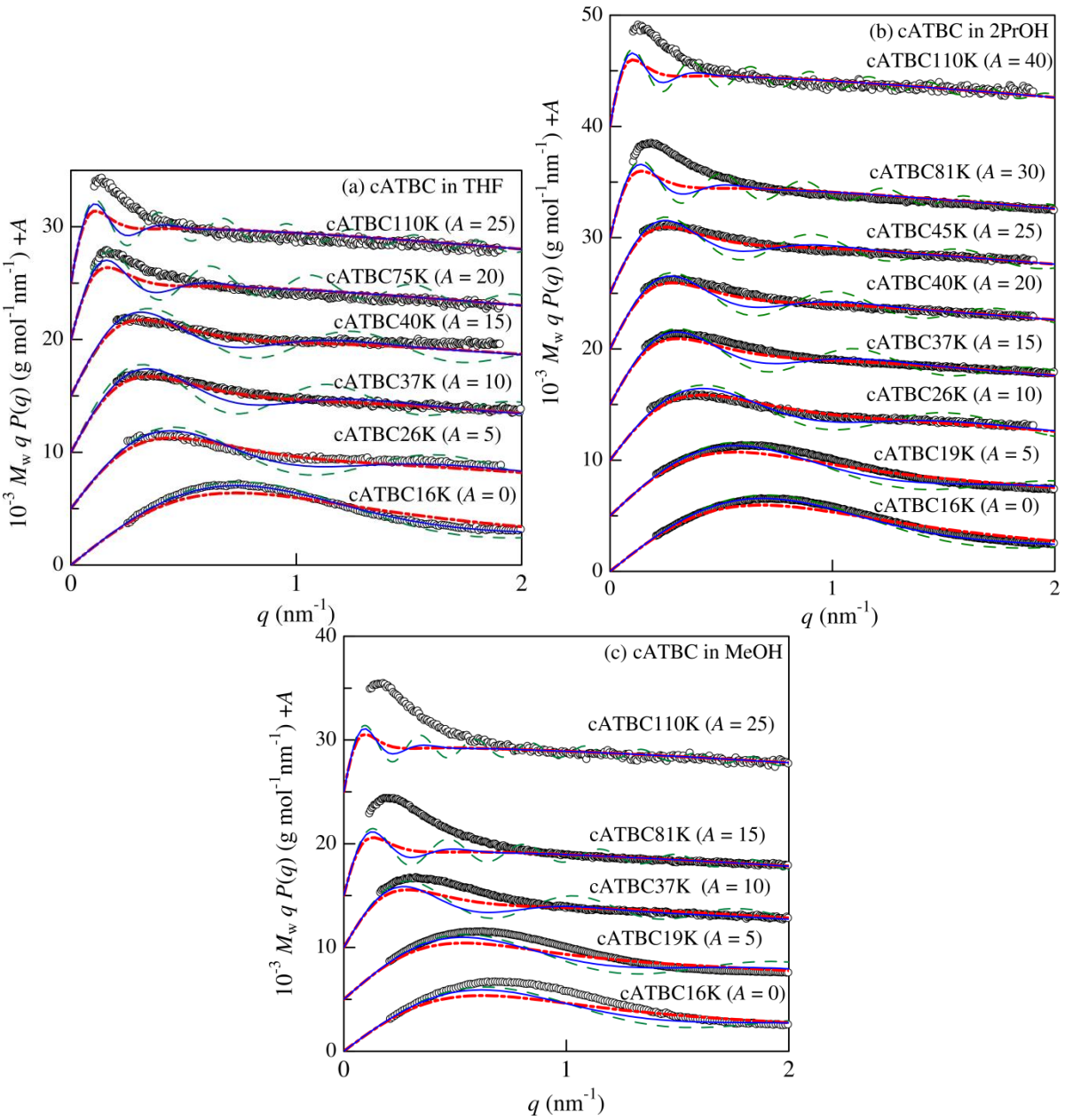

Figure 2. Reduced Holtzer plots for indicated cATBC samples in THF at 25 °C (a), in 2PrOH at 35 °C (b), and in MeOH at 25 °C (c). Dashed (green), solid (blue), and dot-dashed (red) curves, theoretical values for cylindrical rigid rings calculated with the M_L value in Table 2 and with M_w/M_n = 1, 1.05, and 1.2, respectively. The ordinate values are shifted by A for clarity.

Hydrodynamic Properties in 2PrOH at the Theta Temperature. Figure 3 shows the molar mass dependence of the hydrodynamic radius R_H determined from DLS measurements in 2PrOH at 35 °C along with those for cyclic amylose in 0.5 M aqueous NaOH.[14] The data points for cATBC are significantly higher than those for cyclic amylose. This is consistent with the

higher chain stiffness of cATBC than that for amylose. According to Fujii and Yamakawa,[26] R_H for cylindrical wormlike ring can be numerically calculated with the parameters, L, λ, and d when $\lambda L \geq 3.480$. Although this λL range corresponds to $M \geq 1.0 \times 10^5$ for cATBC in 2PrOH, the theoretical solid line in Figure 3 for the wormlike ring with the parameters of M_L = 1500 $nm^{-1}g\ mol^{-1}$, λ^{-1} = 20 nm, and d = 3.2 nm seems to be consistent with the experimental data; it should be noted that the last parameter d was estimated from the intrinsic viscosity data for linear ATBC in the same solvent.[22] Thus, we may conclude that the obtained dimensional and hydrodynamic properties are consistently explained by wormlike ring with substantially the same molecular parameter for the linear ATBC in the same solvent.

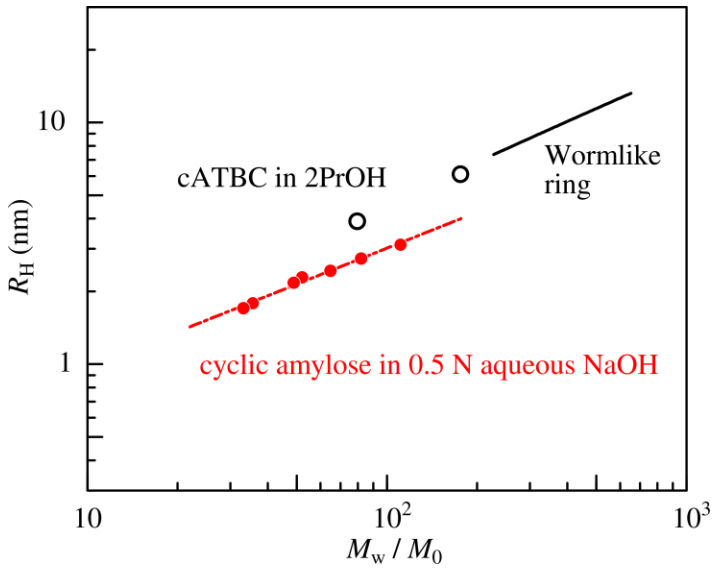

Figure 3. Molar mass dependence of the hydrodynamic radius R_H for cATBC in 2PrOH at 35 °C (unfilled circles) and for cyclic amylose in 0.5 M aqueous NaOH[14] (filled circles). A solid (black) line, theoretical values for cylindrical wormlike ring calculated with M_L = 1500 $nm^{-1}g\ mol^{-1}$, λ^{-1} = 20 nm, and d = 3.2 nm.

Intramolecular Hydrogen Bonds. As discussed in our previous papers,[21-22,24] we showed that the significant solvent dependence of the chain stiffness for linear ATBC can be explained as a function of the number of intramolecular hydrogen bonds of the C=O groups, which is detectable from the waveform separation of the amide I band in the solution IR spectra. As shown in Figure 4, IR spectra for cATBC16K and cATBC19K in 2PrOH, MeOH, and THF are substantially the same as those for linear ATBC in the same solvent, indicating that cATBC has similar intra- and intermolecular hydrogen bonding C=O groups to those for linear one. In THF, amide I band consists of two peaks at 1737 and 1698 cm^{-1}, which corresponds to free and intramolecular hydrogen bonding C=O groups with NH on the neighbor carbamate group. On the other hand, only one broad peak for intermolecular hydrogen bonding with solvent molecules was found in MeOH. Furthermore, those for cATBC in 2PrOH are also nicely fitted by the data for the linear ATBC, in which 29% of C=O groups form intramolecular hydrogen bond with NH groups.[22] Consequently, the number of intramolecular hydrogen bonds increases with the order of MeOH < 2PrOH < THF, and therefore, the high chain stiffness of cATBC is most likely due to the intramolecular hydrogen bonds as is the case with the linear ATBC.

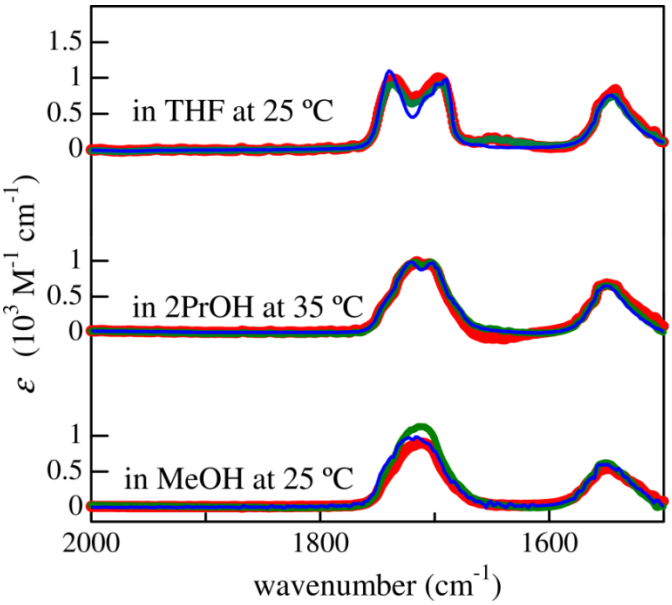

Figure 4. Solution IR spectra in THF at 25 °C, in 2PrOH at 35 °C, and in MeOH at 25 °C for cATBC16K (red), cATBC19K (green) along with those for linear ATBC[21-22] (blue).

Liquid crystallinity. Concentrated solutions of some rigid linear polymers are well known to form anisotropic phase, that is, lyotropic liquid crystal phase. Indeed, we recently found that THF solution of linear ATBC has lyotropic liquid crystallinity.[21] Figure 5 displays polarized light micrographs with a compensator for cATBC45K (c = 0.69 g cm^{-3}) and cATBC75K (c = 0.45 g cm^{-3}). Appreciable color changes as well as transparency under cross-Nicol optical system (not shown here) indicate that not only linear ATBC but also cATBC form lyotropic liquid crystal phase in THF. This may be the first example of liquid crystallinity of rigid ring polymers; it should be noted that a concentrated solution of plasmid shows liquid crystallinity[27] but it forms superhelix, and hence the shape should be rather rodlike. The different color in panels a and b is likely due to the different concentration, but to clarify it, concentration and molar mass dependence should be investigated. This lyotropic liquid crystallinity may be interesting since liquid crystal phase of cyclic polymers should have much different optical characteristics from those consisting of the linear analogue.

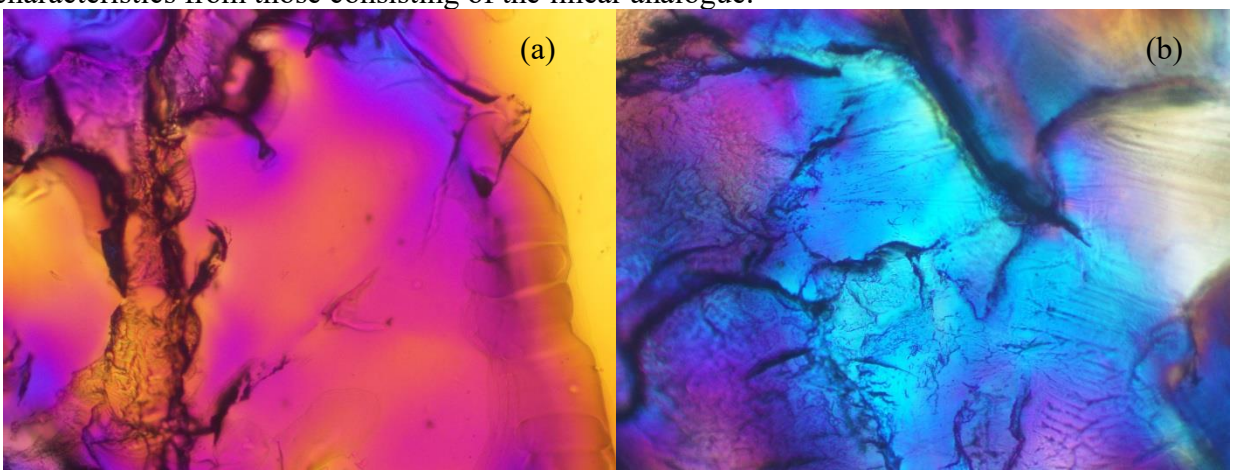

Figure 5. Polarized light micrograph of concentrated THF solutions for (a) cATBC45K (c = 0.69 g cm^{-3}) and (b) cATBC75K (c = 0.45 g cm^{-3}).

Onsager[28] predicted the isotropic-liquid crystal phase equilibrium in solutions of plate-like particles with a diameter D, and calculated the phase boundary concentration c_I between the isotropic and biphasic regions using the second virial approximation. The result is given by

$$c_I = 3.34 \times \left(\frac{4}{\pi}\right)^2 \frac{M}{N_A D^3} \quad (5)$$

where N_A is the Avogadro constant. If cATBC with L is viewed as a plate-like particle with $D = L/\pi$, eq 5 provides us 0.63 g cm^{-3} and 0.23 g cm^{-3} as c_I for cATBC45K and cATBC75K, respectively. While phase boundary concentration cannot be determined due to the limitation of the current sample quantity, only isotropic phase were found at the phase transition concentrations for linear ATBC having similar M_w ($c \sim 0.35 - 0.4$ g cm^{-3}).[29] Thus, the obtained theoretical values are comparable to but seem to be slightly lower than the experimental results. This might be due to the difference between rigid rings and the plate-like particles but there is no corresponding theory for solutions of toroidal particles.

Intermolecular Interactions. Temperature dependence of the second virial coefficient A_2 for cATBC81K and cATBC37K in 2PrOH is shown in Figure 6 along with those for three linear ATBC samples[22] ranging in the molar mass from 7×10^5 to 1.6×10^6. The obtained A_2 for the cATBC samples gradually decreases with lowering temperature and vanishes at 18 °C. Interestingly, this temperature is significantly lower than the theta temperature (35 °C) for linear ATBC at which A_2 for high molar mass linear ATBC vanishes. The A_2 values for cATBC37K and cATBC81K at 35 °C are obtained to be 1.34×10^{-4} mol g^{-2}cm^3 and 1.38×10^{-4} mol g^{-2}cm^3, respectively. Similar positive A_2 for cyclic polymer are reported for polystyrene in cyclohexane.[2,30-31] While the effective binary cluster integral vanishes at theta temperature, that is, repulsive interaction between the two segments for the two polymer chains is in harmony with the attractive interaction, the theta temperature is usually irrespective of the chain architecture. Indeed, the A_2 values for star[32] and comb polystyrenes[33-34] vanish at the theta temperature when the end effects and three segment interactions[35-36] are negligible, that is, except for very low M_w samples. Thus, the positive A_2 in the theta solvent is a characteristic of ring polymers and it is explained by the topological interaction, which is based on that two discrete rings cannot become linked rings without breaking the covalent bonds and this restriction of the spatial arrangement behaves apparently as intermolecular repulsive interactions.[37-38] This effect was investigated theoretically for long flexible ring[39-42] and for rigid ring.[39]

The effective volume V_E to calculate A_2 for rigid rings is formulated as[39]

$$V_E = L^3/24\pi^2 \quad (6)$$

When binary cluster integral of the polymer is negligible, A_2 can be defined using V_E as

$$A_2 = \frac{4N_A V_E}{M^2} = \frac{N_A M}{6\pi^2 M_L^3} \quad (7)$$

Using an average M_L of 1450 nm^{-1}g mol^{-1}, A_2 is calculated to be 1.22×10^{-4} mol g^{-2}cm^3 and 2.70×10^{-4} mol g^{-2}cm^3 for cATBC37K and cATBC81K, respectively. The former is fairly close to that for the experimental value while the latter is appreciably larger. This overestimation of A_2 for cATBC81K is likely due to the flexibility of the chain since $\langle S^2 \rangle_z$ for cATBC81K is appreciably smaller than that calculated for rigid ring while the discrepancy becomes negligibly small for cATBC37K (see Figure 1b). The effective volume V_E for semiflexible ring is recently estimated from Monte Carlo simulation by Ida et al.[8] and they found

that $\lambda V_E/L^2$ ($=A_2\lambda M_L^2/4N_A$) is a function of λL. The resultant simulation data plotted as solid line in Figure 7 fairly fit our experimental A_2 for cATBC, indicating that the positive A_2 can be explained by the topological interaction. It should be noted that the binary cluster integral for the monomer unit of cATBC might be different from that for linear ATBC owing to the high chain stiffness. Therefore, the difference may cause A_2 appreciably, suggesting ring polymers having high chain stiffness might not be very suitable to confirm the theories.

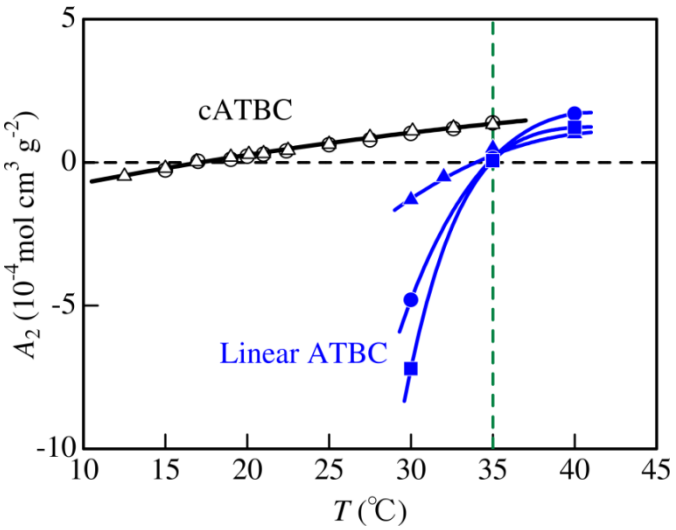

Figure 6. Temperature dependence of the second virial coefficients A_2 for cATBC81K (unfilled circles) and cATBC37K (unfilled triangles) in 2PrOH, along with A_2 for three linear ATBC samples,[22] of which M_w's are 6.94×10^5 (filled circles), 8.89×10^5 (filled squares), and 1.61×10^6 (filled triangles).

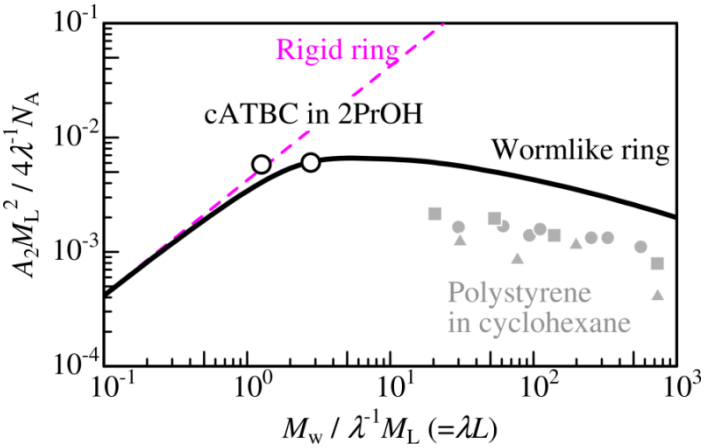

Figure 7. Reduced chain length ($\lambda L = M_w/\lambda^{-1}M_L$) dependence of the reduced second virial coefficient ($A_2M_L^2/4\lambda^{-1}N_A$) for cATBC in 2PrOH (unfilled circles) at the theta temperature (35 °C) along with those for polystyrene in cyclohexane (filled circles, Roovers et al.;[2] filled triangles, Huang et al.;[30] filled squares, Takano et al.[31]) at the theta temperature (34.5 – 35 °C). Solid curve, results from Monte Carlo simulation by Ida et. al.[8] Dashed line, theoretical values for rigid ring.[39]

■ CONCLUSIONS

Although limited available theories for dimensional and hydrodynamic properties for ring polymers except for the radius of gyration, they are successfully explained by the current theories for wormlike ring in the available range of the theories. This indicates that cATBC behaves as rigid ring stabilized by the intramolecular hydrogen bonds and the Kuhn segment length is as large as 75 nm for linear ATBC in THF and becomes more flexible in alcohols, that is, 20 nm in 2PrOH and 11 nm in MeOH. The positive second virial coefficient in the theta solvent, 2PrOH at 35°C, is well explained by a current theory considering intermolecular topological interactions.

■ ASSOCIATED CONTENT

Supporting Information

Some examples of raw SAXS and DLS data, theoretical and experimental plots for SAXS, and $<S^2>_z - M_w$ plots for cATBC in the three solvents. This material is available free of charge via the Internet at http://pubs.acs.org.

■ AUTHOR INFORMATION

Corresponding Author

*E-mail: kterao@chem.sci.osaka-u.ac.jp

Notes

The authors declare no competing financial interest.

■ ACKNOWLEDGMENTS

The synchrotron radiation experiments were performed at the BL40B2 in SPring-8 with the approval of the Japan Synchrotron Radiation Research Institute (JASRI) (Proposal Nos. 2011A1049 and 2011B1068) and at the BL-10C in KEK-PF under the approval of the Photon Factory Program Advisory Committee (Nos. 2010G080 and 2011G557). The authors thank Prof. Yoji Inoko (Osaka Univ.) for SAXS measurements in KEK-PF. This work was partially supported by JSPS KAKENHI Grant No. 23750128.

Dedication

Dedicated to Professor Emeritus Takashi Norisuye on the occasion of his 70th birthday.

■ REFERENCES

(1) Dodgson, K.; Sympson, D.; Semlyen, J. A. *Polymer* **1978**, *19*, 1285-1289.

(2) Roovers, J.; Toporowski, P. M. *Macromolecules* **1983**, *16*, 843-849.

(3) Yamamoto, T.; Tezuka, Y. *Polym. Chem.* **2011**, *2*, 1930-1941.

(4) Kricheldorf, H. R. *J. Polym. Sci., Part A: Polym. Chem.* **2010**, *48*, 251-284.

(5) Laurent, B. A.; Grayson, S. M. *Chem. Soc. Rev.* **2009**, *38*, 2202-2213.

(6) Endo, K. In *New Frontiers in Polymer Synthesis*; Kobayashi, S., Ed.; Springer-Verlag Berlin: Berlin, 2008; Vol. 217, p 121-183.

(7) Yamakawa, H. *Helical Wormlike Chains in Polymer Solutions*; Springer: Berlin, Germany, 1997.

(8) Ida, D.; Nakatomi, D.; Yoshizaki, T. *Polym. J.* **2010**, *42*, 735-744.

(9) Schappacher, M.; Deffieux, A. *Science* **2008**, *319*, 1512-1515.

(10) Rzayev, J. *ACS Macro Lett.* **2012**, *1*, 1146-1149.

(11) Terao, K.; Asano, N.; Kitamura, S.; Sato, T. *ACS Macro Lett.* **2012**, *1*, 1291-1294.
(12) Kitamura, S.; Isuda, H.; Shimada, J.; Takada, T.; Takaha, T.; Okada, S.; Mimura, M.; Kajiwara, K. *Carbohydr. Res.* **1997**, *304*, 303-314.
(13) Shimada, J.; Kaneko, H.; Takada, T.; Kitamura, S.; Kajiwara, K. *J. Phys. Chem. B* **2000**, *104*, 2136-2147.
(14) Nakata, Y.; Amitani, K.; Norisuye, T.; Kitamura, S. *Biopolymers* **2003**, *69*, 508-516.
(15) Takaha, T.; Yanase, M.; Takata, H.; Okada, S.; Smith, S. M. *J. Biol. Chem.* **1996**, *271*, 2902-2908.
(16) Shimada, J.; Yamakawa, H. *Biopolymers* **1988**, *27*, 657-673.
(17) Terao, K.; Fujii, T.; Tsuda, M.; Kitamura, S.; Norisuye, T. *Polym. J.* **2009**, *41*, 201-207.
(18) Nakanishi, Y.; Norisuye, T.; Teramoto, A.; Kitamura, S. *Macromolecules* **1993**, *26*, 4220-4225.
(19) Fujii, T.; Terao, K.; Tsuda, M.; Kitamura, S.; Norisuye, T. *Biopolymers* **2009**, *91*, 729-736.
(20) Tsuda, M.; Terao, K.; Nakamura, Y.; Kita, Y.; Kitamura, S.; Sato, T. *Macromolecules* **2010**, *43*, 5779-5784.
(21) Terao, K.; Murashima, M.; Sano, Y.; Arakawa, S.; Kitamura, S.; Norisuye, T. *Macromolecules* **2010**, *43*, 1061-1068.
(22) Sano, Y.; Terao, K.; Arakawa, S.; Ohtoh, M.; Kitamura, S.; Norisuye, T. *Polymer* **2010**, *51*, 4243-4248.
(23) Burchard, W. *Polymer* **1969**, *10*, 467-475.
(24) Arakawa, S.; Terao, K.; Kitamura, S.; Sato, T. *Polym. Chem.* **2012**, *3*, 472-478.
(25) Nakata, Y.; Norisuye, T.; Kitamura, S. *Biopolymers* **2002**, *64*, 72-79.
(26) Fujii, M.; Yamakawa, H. *Macromolecules* **1975**, *8*, 792-799.
(27) Zakharova, S. S.; Jesse, W.; Backendorf, C.; van der Maarel, J. R. *Biophys J* **2002**, *83*, 1119-1129.
(28) Onsager, L. *Ann. N. Y. Acad. Sci.* **1949**, *51*, 627-659.
(29) Oyamada, K.; Terao, K.; Suwa, M.; Kitamura, S.; Sato, T. *Macromolecules* **2013**, *46*, 4589-4595.
(30) Huang, J. X.; Shen, J.; Li, C. R.; Liu, D. Z. *Makromol. Chem. Macromol. Chem. Phys.* **1991**, *192*, 1249-1254.
(31) Takano, A.; Kushida, Y.; Ohta, Y.; Masuoka, K.; Matsushita, Y. *Polymer* **2009**, *50*, 1300-1303.
(32) Okumoto, M.; Terao, K.; Nakamura, Y.; Norisuye, T.; Teramoto, A. *Macromolecules* **1997**, *30*, 7493-7499.
(33) Terao, K.; Takeo, Y.; Tazaki, M.; Nakamura, Y.; Norisuye, T. *Polym. J.* **1999**, *31*, 193-198.
(34) Terao, K.; Nakamura, Y.; Norisuye, T. *Macromolecules* **1999**, *32*, 711-716.
(35) Nishi, Y.; Nakamura, Y.; Norisuye, T. *Polym. J.* **2009**, *41*, 58-62.
(36) Mizuno, T.; Terao, K.; Nakamura, Y.; Norisuye, T. *Macromolecules* **2005**, *38*, 4432-4437.
(37) Edwards, S. F. *Proc. Phys. Soc., London* **1967**, *91*, 513-&.
(38) Edwards, S. F. *J. Phys. A: Gen. Phys.* **1968**, *1*, 15.
(39) des Cloizeaux, J. *J. Phys., Lett.* **1981**, *42*, L433-L436.

(40) Iwata, K.; Kimura, T. *J. Chem. Phys.* **1981**, *74*, 2039-2048.
(41) Iwata, K. *Macromolecules* **1985**, *18*, 115-116.
(42) Tanaka, F. *J. Chem. Phys.* **1987**, *87*, 4201-4206.

For Table of Contents Use Only

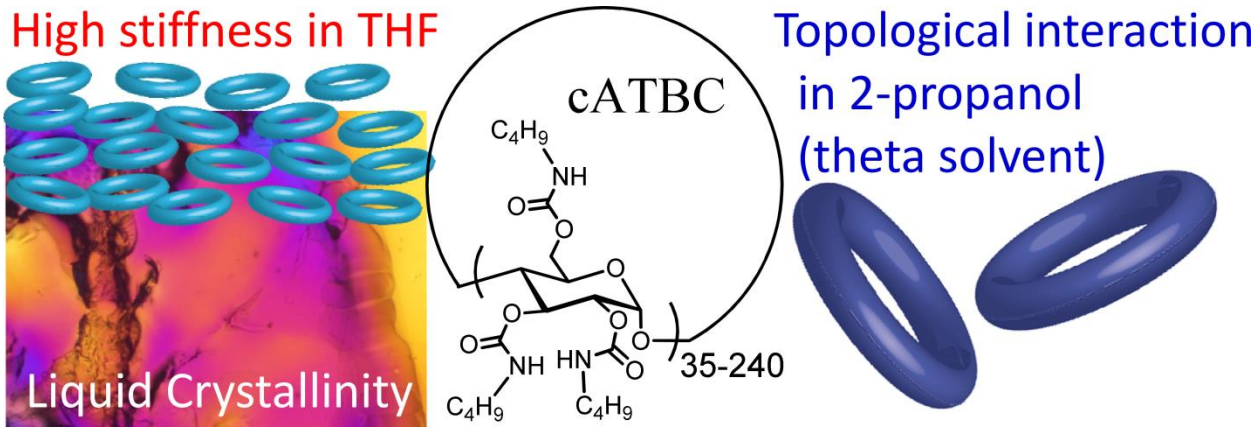

Solution Properties of a Cyclic Chain Having Tunable Chain Stiffness: Cyclic Amylose Tris(*n*-butylcarbamate) in Theta and Good Solvents

Ken Terao*, Kazuya Shigeuchi, Keiko Oyamada, Shinichi Kitamura, Takahiro Sato